Effect of Nickel Doping on the Physical and Sensing Properties of Titanium Dioxide Nanostructures via Chemical Spray Pyrolysis

Murtada Kudhier Abbas Hassan[1], Taghreed Khalid Hameed[2], Ali Mohammed Jabbar[3], Shaymaa A. Hussein[4] and Nabeel Mubarak Mirza[2]
[1]*Department of Scientific Affairs, Mustansiriyah University, 10052 Baghdad, Iraq*
[2]*Department of Physics, College of Education, Mustansiriyah University, 10052 Baghdad, Iraq*
[3]*Department of Physics, College of Science, Mustansiriyah University, 10052 Baghdad, Iraq*
[4]*Department of Medical Laboratory Techniques, Al-Manara College for Medical Sciences, 62001 Amarah, Iraq*
nabeel.mirza@uomustansiriyah.edu.iq

Keywords: Titanium Dioxide, Thin Films, Nickel Doping, CSP, XrD, Surface Finish, E_g, Gas Sensing.

Abstract: In this work, Chemical spray pyrolysis (CSP) was used for producing nickel-doped TiO_2 nanostructured thin films with a thickness of ~330 nm. XRD analysis confirmed a polycrystalline anatase phase with preferential orientation along the (004) plane. Crystallite size increased from 11.53 nm for pure TiO_2 to 24.32 nm for TiO_2:3% Ni. Dislocation density and lattice strain decreased, indicating improved crystalline quality as the dopant increased. AFM revealed that Ni doping increases the average particle size and reduces topography parameters, suggesting modified surface morphology and grain distribution. UV–Vis spectroscopy showed high transparency (90–95%) in the visible range and a decrease in band gap from 3.50 eV for undoped TiO_2 to 3.40 eV for 3% Ni-doped films, attributed to defect states introduced by Ni. Gas-sensing measurements toward NO_2 at 100 °C showed a decrease in sensitivity with increasing Ni content, from 35.22% for pure TiO_2 to 12.14% for TiO_2:3% Ni at 200 ppm, likely due to altered charge-carrier transport. In general, adding Ni changes the physical properties of TiO_2 thin films, showing they could be useful for gas sensors.

1 INTRODUCTION

Titanium dioxide (TiO_2) has garnered significant attention due to its superior chemical and physical characteristics [1]. These include non-toxicity [2], excellent chemical stability [3], affordability [4], a high dielectric constant [5], a refractive index [6], and optical clarity in the visible spectrum [7]. Due to these properties, TiO_2 has found extensive use in many technological fields such as pigments [8], gas sensors [9], photocatalysts [10], dye-sensitized solar cells [11], optical waveguides [12], optical amplifiers [13], optoelectronic detectors [14], and TiO_2–SiO_2 Bragg mirrors [15]. Doping TiO_2 thin films with transition-metal ions like Ni, Zn, Cu, Fe, Cr, and Co has been found to improve their photocatalytic efficiency [16]. This improvement is usually associated with defects in the TiO_2 structure, such as interstitial atoms or substitutional ions, vacancies, or composite oxides [17]. The high surface-to-volume ratio and strong interactions with gas molecules have prompted significant interest in gas-sensing schemes employing TiO_2 nanostructures [18]. More closely, the sensing mechanism of TiO_2-based materials is predominantly due to changes in electrical resistance arising from gas species adsorption and desorption on the sensing layer surface [19]. It is known that transition metals such as Ni positively influence sensing performance through electronic-structure changes, oxygen-vacancy enrichment, and enhanced surface charge transfer upon TiO_2 doping [20]. Through such modifications, sensitivity, selectivity, and response–recovery parameters are improved, rendering doped TiO_2 nanostructures potential candidates for applications in environmental monitoring and gas detection [21], [22]. The present work aims to synthesize Ni-doped TiO_2 nanostructures via chemical spray pyrolysis in a systematic manner to characterize how nickel incorporation affects all the parameters under investigation.

2 EXPERIMENTAL

CSP was applied to lay thin films of TiO_2:Ni. The solution was sprayed using a glass atomizer. At 400 °C, films were formed on glass bases. Redistilled water was used to dissolve 0.1 M of $NiCl_2$ (Sigma Aldrich UK) and $TiCl_3$ (Merck Chemicals Germany). Nickel was used at volumetric concentrations of 1% and 3%. The best results were obtained at 8 second spray duration and a one-minute break between pass ups. The pressure of the transport gas (air) was set to 10^5 Pa, resulting in a 30 cm gap between the base and the spout. Gravimetric measurements indicated a film thickness of approximately 330 nm. XRD (Shimadzu XRD-6000, Japan) was used for calculating structural coefficients. Surface topography is studied using an AFM (AA 3000 scanning probe microscope). Gas response was determined by the change in electrical resistance of the sensing film within a 8 cm radius by 17 cm high cylindrical chamber.

3 RESULTS AND DISCUSSION

Figure 1 presents the X-ray diffraction (XRD) patterns of the fabricated TiO_2 and Ni-doped TiO_2 thin films with a thickness of 325 nm. The diffraction patterns exhibit several well-defined peaks corresponding to the anatase phase of TiO_2. The observed reflections are indexed to the (101), (004), (105), and (204) crystallographic planes located at diffraction angles of 25.30°, 37.75°, 53.82°, and 62.58°, respectively. Among these reflections, the (004) plane exhibits the highest intensity, indicating a preferred growth orientation. The diffraction peaks are in excellent agreement with ICDD card No. 21-1272, confirming the successful formation of polycrystalline anatase TiO_2 thin films. A slight shift in the diffraction peak positions is observed with increasing Ni concentration, indicating the successful incorporation of Ni ions into the TiO_2 lattice. This shift is attributed to lattice distortion resulting from the substitution of Ti^{4+} ions by Ni ions with different ionic radii [8].

The structural parameters obtained from the XRD analysis are summarized in Table 1. The crystallite size increases from 11.53 nm for the undoped TiO_2 film to 19.73 nm and 24.32 nm for the films containing 1% and 3% Ni, respectively. These results indicate that increasing the nickel concentration promotes grain growth and improves the crystallinity of the deposited films [4]. The enhancement in crystallite size also suggests better structural ordering of the Ni-doped TiO_2 films, which can be attributed to dopant-induced lattice modification that facilitates atomic rearrangement and reduces lattice defects [25].

The dislocation density decreases from 49.2×10^{14} to 30.86×10^{14} lines/m² with increasing Ni concentration, indicating a reduction in crystal defects and an improvement in crystalline quality [26], [27]. Likewise, the microstrain decreases from 37.45×10^{-4} to 26.32×10^{-4}, reflecting reduced lattice distortion and enhanced structural stability of the deposited films [28], [29]. The structural parameters are summarized in Table 1, while Figure 2 illustrates the variation of FWHM, crystallite size, dislocation density, and microstrain as a function of Ni concentration.

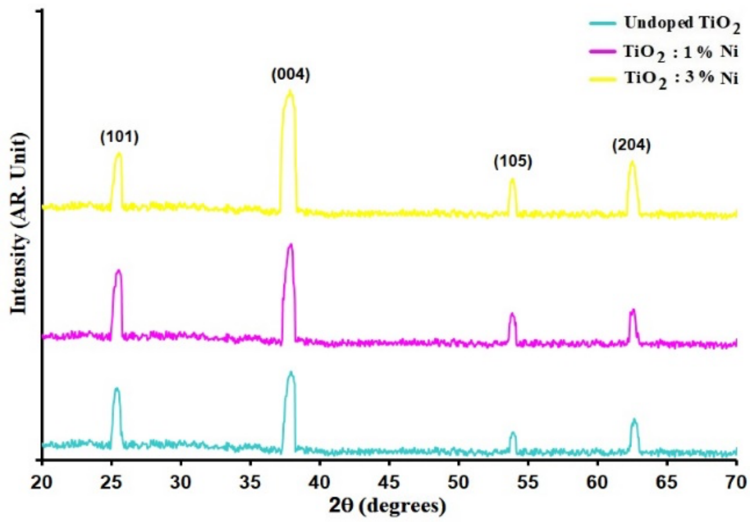

Figure 1: X-ray diffraction (XRD) patterns of pure and Ni-doped TiO_2 thin films.

Table 1: *D*, E_g, and S_{para} of TiO_2:Ni films.

Sample	(hkl) Plane	2 θ (°)	FWHM (°)	E_g (eV)	*D* (nm)	δ (× 10^{14}) (lines/m^2)	ε (× 10^{-4})
TiO_2	004	37.75	0.72	3.50	11.53	49.2	37.45
TiO_2: 1% Ni	004	37.41	0.67	3.45	19.73	37.38	35.91
TiO_2: 3% Ni	004	37.38	0.62	3.40	24.32	30.86	26.32

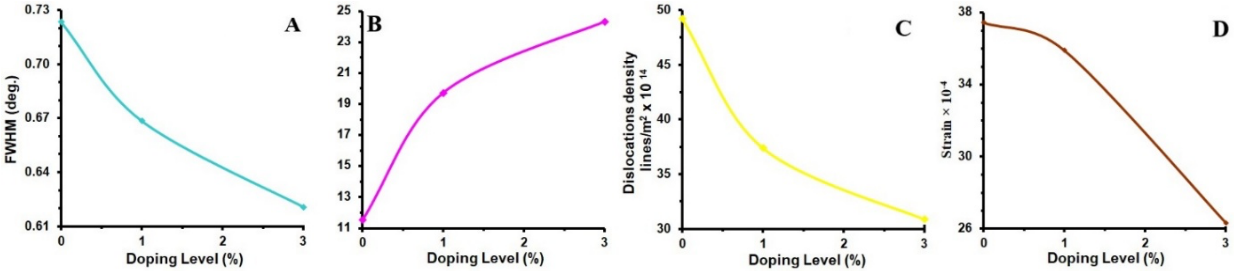

Figure 2: Structural parameters of the deposited TiO_2 thin films: a) FWHM, b) crystallite size (D), c) dislocation density (δ), and d) microstrain (ε).

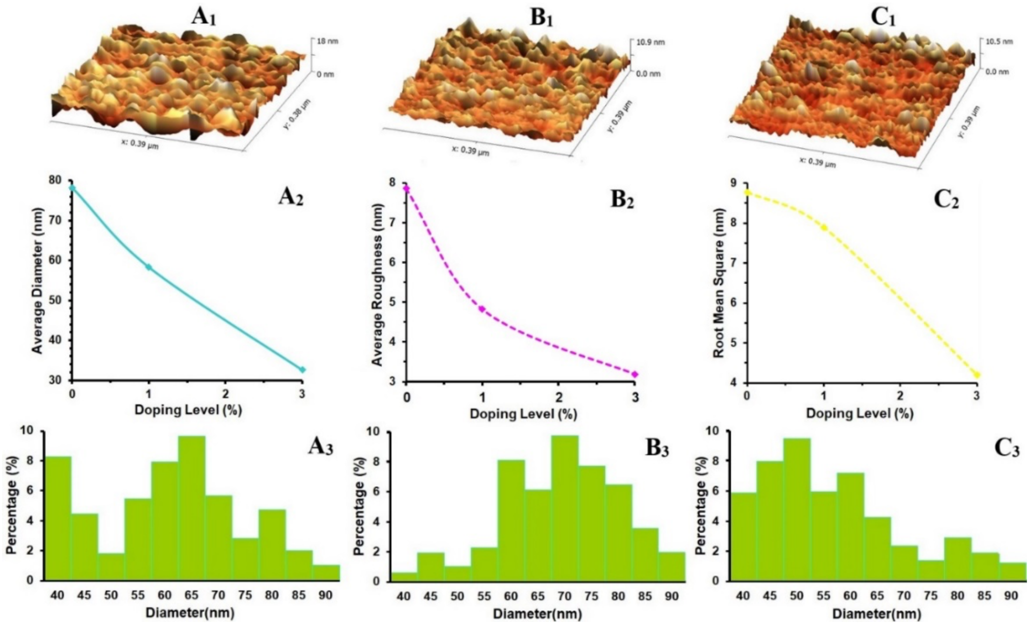

Figure 3: AFM surface parameters of pure and Ni-doped TiO_2 thin films.

The surface morphology of the deposited films was investigated using atomic force microscopy (AFM), and the corresponding images are presented in Figure 3. The AFM parameters are summarized in Table 2. The average particle size increases from 32.6 nm for pure TiO_2 to 58.3 nm and 78.2 nm for the films doped with 1% and 3% Ni, respectively. In contrast, both the average roughness (Ra) and the root-mean-square (RMS) roughness decrease with increasing Ni concentration, indicating that nickel incorporation produces smoother and more homogeneous film surfaces.

The optical transmittance spectra of the deposited films are presented in Figure 4. All films exhibit high optical transparency in the visible region, with transmittance values ranging from approximately 90.5% to 95.5%. Furthermore, the transmittance increases toward longer wavelengths, indicating reduced optical absorption in the near-infrared region. This behavior is attributed to the relatively wide optical band gap of TiO_2 and the lower probability of electronic transitions at lower photon energies [18].

Table 2: AFM TiO_2-Ni film parameters.

Sample	P_{av} (nm)	Ra (nm)	rms (nm)
TiO_2	32.6	7.87	8.76
TiO_2: 1% Ni	58.3	4.82	7.89
TiO_2: 3% Ni	78.2	3.19	4.20

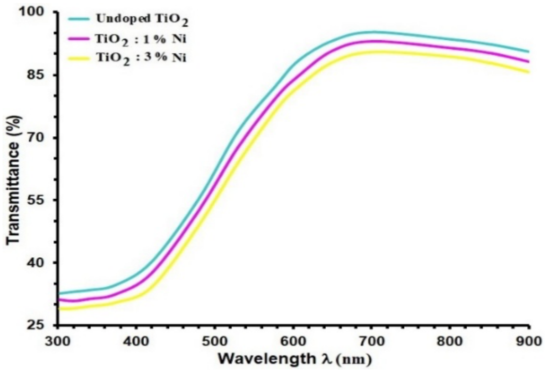

Figure 4: Optical transmittance spectra of pure and Ni-doped TiO_2 thin films.

Figure 5 presents the optical absorbance spectra of the pure and Ni-doped TiO_2 thin films. The absorbance increases progressively with increasing Ni concentration, while the undoped TiO_2 film exhibits the lowest absorbance. The enhanced optical absorption is mainly attributed to the incorporation of nickel ions, which introduce additional localized energy states within the TiO_2 band structure and facilitate optical transitions [32], [33].

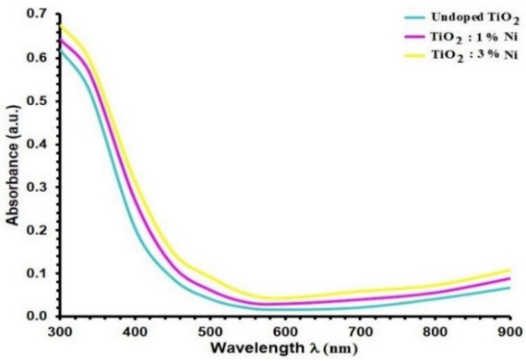

Figure 5: Optical absorbance spectra of pure and Ni-doped TiO_2 thin films.

Figure 6 illustrates the absorption coefficient spectra of the deposited films. The absorption coefficient increases with increasing nickel concentration, indicating improved photon absorption after Ni incorporation [34], [35]. A sharp increase is observed near the absorption edge owing to direct electronic transitions, whereas a gradual decrease occurs at higher photon energies. The increase in the absorption coefficient is attributed to modifications in the electronic structure caused by nickel incorporation, which introduces localized defect states within the band gap [36], [37].

The optical band gap values are presented in Figure 7. The band gap decreases gradually from 3.50 eV for the undoped TiO_2 film to approximately 3.40 eV for the film containing the highest Ni concentration. This reduction is attributed to impurity and defect states introduced by nickel incorporation, which create additional energy levels within the forbidden band gap and facilitate electronic transitions at lower photon energies [38], [39]. The observed band-gap narrowing is also associated with structural disorder and defect formation induced by Ni doping [40], [41].

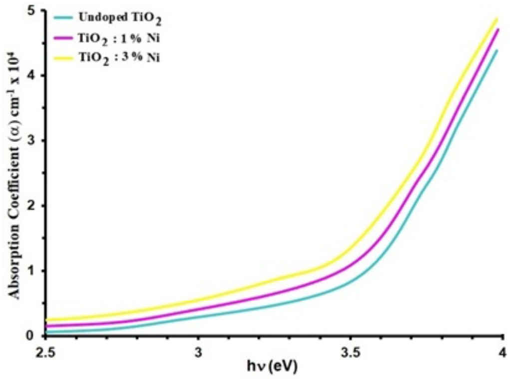

Figure 6: Absorption coefficient spectra of pure and Ni-doped TiO_2 thin films.

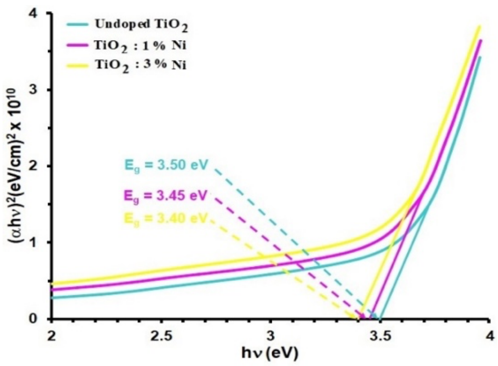

Figure 7: Optical band gap of pure and Ni-doped TiO_2 thin films.

Figure 8 shows the extinction coefficient spectra of the deposited films. The extinction coefficient increases rapidly in the ultraviolet region and gradually decreases with increasing wavelength [42], [43]. The non-zero extinction coefficient below the fundamental absorption edge indicates the presence of defect and impurity states that contribute to sub-band-gap optical absorption [44]–[47].

The variation of the refractive index with wavelength is presented in Figure 9. The refractive index decreases systematically with increasing nickel concentration throughout the investigated spectral range. This behavior is attributed to changes in the electronic polarizability and structural properties of the films resulting from the incorporation of nickel into the TiO_2 lattice [48], [49]. Similar behavior has been reported in previous studies of Ni-doped TiO_2 thin films [50]–[53].

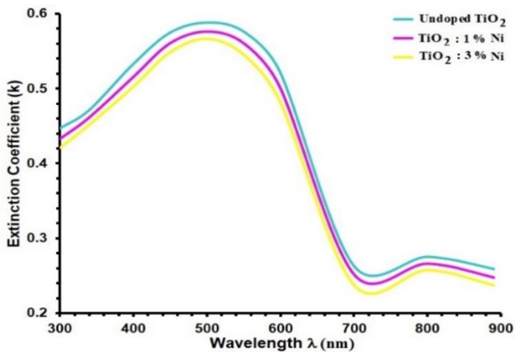

Figure 8: Extinction coefficient spectra of pure and Ni-doped TiO_2 thin films.

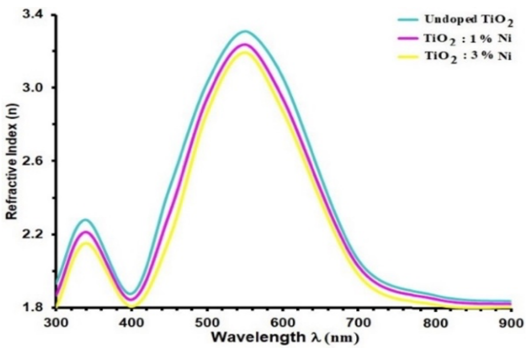

Figure 9: Refractive index spectra of pure and Ni-doped TiO_2 thin films.

The gas-sensing performance of the fabricated films was evaluated at an operating temperature of 100 °C. Figure 10 presents the dynamic resistance response of the pure and Ni-doped TiO_2 thin films upon exposure to 200 ppm NO_2 gas. The undoped TiO_2 film exhibits the lowest electrical resistance, indicating more efficient adsorption of NO_2 molecules on its surface [54]–[56]. In contrast, the electrical resistance increases with increasing Ni concentration, reaching its highest value for the film containing 3% Ni. This behavior is attributed to changes in the electronic structure and charge-transport mechanism caused by nickel incorporation, which reduce charge-carrier mobility and modify the interaction between the sensing surface and NO_2 molecules [57]–[60].

Figure 11 illustrates the NO_2 gas-sensing sensitivity of the pure and Ni-doped TiO_2 thin films. The sensitivity decreases systematically with increasing nickel concentration [61], [62]. Specifically, the sensitivity decreases from 35.22% to 12.14% at 200 ppm, from 37.14% to 13.27% at 150 ppm, and from 38.54% to 14.53% at 300 ppm as the Ni concentration increases from 0% to 3%. This reduction in sensitivity is attributed to changes in the electronic structure and enhanced charge-carrier recombination, which reduce the number of free carriers available for gas detection and consequently weaken the sensing performance of the TiO_2 thin films [63], [64].

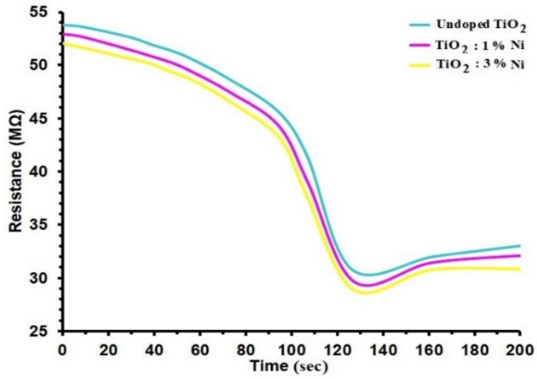

Figure 10: Electrical resistance response of pure and Ni-doped TiO_2 thin films toward NO_2 gas.

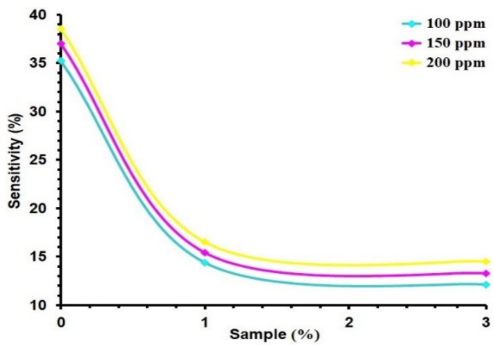

Figure 11: Sensitivity of pure and Ni-doped TiO_2 thin films toward NO_2 gas.

4 CONCLUSIONS

CSP was used to deposit both undoped and nickel-doped TiO_2 thin films (1% and 3% Ni). A polycrystalline anatase structure with a preferred (004) orientation was verified by XRD investigation. For undoped films, crystallite size was 11.53 nm; for 3% Ni-doped films, it was 24.32 nm. The decrease in dislocation density and lattice strain indicates enhanced crystalline quality and reduced structural defects. AFM investigations revealed substantial surface modifications, with both average roughness and mean particle diameter decreasing as nickel content increased, confirming nickel's crucial role in tailoring surface morphology. Optical measurements showed high visible transparency (90.5–95.5%) and an increased absorption coefficient upon doping. The optical band gap narrowed from 3.50 eV to 3.40 eV with 3% Ni doping, ascribed to the development of localized energy states within the band gap. Gas-sensing measurements toward 200 ppm NO_2 at 100°C revealed that nickel doping significantly influences the electrical properties [65]. The 3% Ni-doped film exhibited the highest resistance, while sensitivity decreased from 35.22% to 12.14% as Ni content increased.

ACKNOWLEDGMENTS

Mustansiriyah University (www.uomustansiriyah.edu.iq) supports this effort.

REFERENCES

[1] M. Al Saleh, "A Review of the Synthesis, Structural, and Optical Properties of TiO_2 Nanoparticles: Current State of the Art and Potential Applications," Crystals, vol. 15, no. 11, 944, 2025.

[2] Y. S. Bukichev, L. M. Bogdanova, V. A. Lesnichaya, N. V. Chukanov, N. D. Golubeva, and G. I. Dzhardimalieva, "Mechanical and thermophysical properties of epoxy nanocomposites with titanium dioxide nanoparticles," Applied Sciences, vol. 13, no. 7, 4488, 2023.

[3] R. Ali and A. H. Alwan, "Titanium dioxide nanoparticles in dentistry: Multifaceted applications and innovations," Future Dental Research, vol. 1, no. 1, pp. 12-25, 2023.

[4] P. Gangwar and N. K. Sharma, "On the performance of indium tin oxide and titanium dioxide based plasmonic sensor: a theoretical evaluation," Optical Engineering, vol. 65, no. 2, 027101, 2026.

[5] G. K. Podagatlapalli, T. Jena, S. Maddila, S. Hamad, S. Vadavalli, C. Angani, and V. R. Soma, "Single-beam femtosecond Z-scan studies of bismuth and manganese co-doped titanium dioxide nanoparticles dispersed in ethanol," RSC Advances, vol. 16, no. 12, pp. 11023-11035, 2026.

[6] A. Hassein-Bey, N. Belgroune, A. Bessi, O. Kebour, M. Mohammedi, A. R. Touil, and A. Boudjemaa, "Structural Characterization and Photocatalytic Performance of PDMS/TiO_2 Nanocomposites Prepared via Ex Situ Dispersion Route," Applied Mechanics, vol. 7, no. 1, 18, 2026.

[7] K. Nagaraj, S. Radha, C. G. Deepa, K. Raja, V. Umapathy, N. P. Badgujar, et al., "Photocatalytic advancements and applications of titanium dioxide (TiO_2): Progress in biomedical, environmental, and energy sustainability," Next Research, vol. 2, no. 1, 100180, 2025.

[8] K. Drozdowska and J. Smulko, "Selective light-activation of sensing regions in hybrid Au-graphene-TiO_2 chemiresistive gas sensor," Sensors and Actuators B: Chemical, vol. 437, 137764, 2025.

[9] X. N. Qi, Y. Q. Zhu, H. Yuan, Z. X. Xu, H. R. Guo, and Z. L. Li, "Latest progress based on doped-TiO_2 photocatalysis materials: Fabrication and applications," Journal of Water Process Engineering, vol. 78, 108791, 2025.

[10] F. N. Almutairi, A. Ghitas, H. Alanazi, and M. A. Shahat, "Gamma-irradiated Chitosan@PVA@TiO_2 catalytic counter electrodes for enhanced dye-sensitized solar cell (DSSC) performance," Synthetic Metals, vol. 311, 117841, 2025.

[11] Y. Lu, D. Zhang, K. Guo, M. Sun, G. Yuan, S. Zhao, and X. Gu, "Surface modification of TiO_2 nanoparticles doped in photocured resins for the high refractive index optical waveguide," Applied Surface Science, vol. 686, 162186, 2025.

[12] A. Herrera, F. Londoño, and N. M. Balzaretti, "Structural and optical properties of Nd^{3+} doped GeO_2-PbO glass modified by TiO_2 for applications in laser and fiber amplifier," Optical Materials, vol. 113, 110884, 2021.

[13] S. Ge, D. Sang, L. Zou, Y. Yao, C. Zhou, H. Fu, et al., "A review on the progress of optoelectronic devices based on TiO_2 thin films and nanomaterials," Nanomaterials, vol. 13, no. 7, 1141, 2023.

[14] F. Latreche, R. Bensaha, N. Daldosso, A. Romeo, and F. Enrichi, "Nd-doped SiO_2/TiO_2 Bragg reflectors produced by sol-gel dip-coating deposition," Journal of Sol-Gel Science and Technology, vol. 116, no. 2, pp. 1389-1400, 2025.

[15] S. Waseem, T. Zeeshan, H. Tariq, F. Majid, M. D. Ali, Z. N. Kayani, and M. Amami, "The influence of transition metals (Fe, Co) on the structural, magnetic and optical properties of TiO_2 nanoparticles synthesized by the hydrothermal method," Applied Physics A, vol. 128, no. 8, 690, 2022.

[16] D. Dambournet, "Cationic vacancies in anatase (TiO_2): synthesis, defect characterization, and ion-intercalation properties," Accounts of Chemical Research, vol. 55, no. 5, pp. 696-706, 2022.

[17] M. A. Belgami and C. S. Rout, “NO_2 Gas Sensors Based on MXenes,” in MXene Based Gas Sensors, CRC Press, pp. 164-178, 2026.

[18] K. V. Arundhathi, N. John, T. Abraham, K. G. Ambady, and B. Mathew, “Smart nanomaterials for sustainable green energy applications: environmental technology and sustainability,” in Environmental Technology and Sustainability, Apple Academic Press, pp. 259-282, 2024.

[19] A. Tahir, M. A. Bujran, M. Rafiq, S. Irfan, J. Farooq, F. A. Sheikh, and B. Want, “Nickel-doped TiO_2 Nanofibers: A bifunctional material for sustainable hydrogen production and chromium (VI) sensing,” Journal of Power Sources, vol. 664, 238950, 2026.

[20] S. S. Scindia and P. N. Dange, “Redox-tuned core-shell Au nanoparticles encapsulated in benzene sulphonic acid-doped polypyrrole for multiplexed toxic gas detection,” Journal of Nanoparticle Research, vol. 28, no. 2, 46, 2026.

[21] N. H. Thang and N. C. Hien, “Environmental and energy applications of green-synthesized semiconductor nanomaterials: from photocatalysis to smart sensors,” Ionics, pp. 1-36, 2026.

[22] M. M. Seker Perez, C. Boyraz, and L. Arda, “Synthesis, structure, and magnetic properties of (Co/Ce) co-doped ZnO nanoparticles,” Journal of Materials Science: Materials in Electronics, vol. 37, no. 5, 392, 2026.

[23] M. A. Issa and K. A. Aadim, “Optical and structural characterization of ZnO:NiO nano composite prepared by pulsed laser deposition method,” Journal of Optics, vol. 54, pp. 2357-2362, 2025.

[24] T. H. Mubarak, K. H. Hassan, and Z. M. A. Abbas, “Using X-ray diffraction and scanning electron microscope to study zinc oxide nanoparticles prepared by wet chemical method,” Advanced Materials Research, vol. 685, pp. 119-122, 2013.

[25] S. Panda and S. K. Parida, “Studies on structural, microstructural, dielectric, electrical, and optical properties of Gd-doped $BiFeO_3$ ceramics and NTC thermistor application,” Materials Advances, 2026.

[26] S. Göktaş and G. Şahin, “Impact of different Cu sources on the structure, surface morphology, optical and photocatalytic characteristics of sol-gel derived CuO thin films,” Türk Doğa ve Fen Dergisi, vol. 14, no. 1, pp. 13-20, 2025.

[27] R. S. Ali, H. S. Rasheed, N. F. Habubi, and S. S. Chiad, “Synthesis and characterization of manganese-doped FeS_2 thin films via chemical spray pyrolysis,” Chalcogenide Letters, vol. 20, no. 1, pp. 63-72, 2023.

[28] P. C. Chou, H. I. Chen, I. P. Liu, C. C. Chen, J. K. Liou, K. S. Hsu, and W. C. Liu, “On the ammonia gas sensing performance of a RF sputtered NiO thin-film sensor,” IEEE Sensors Journal, vol. 15, no. 7, pp. 3711-3715, 2015.

[29] D. M. Shaker, R. R. Ahmed, A. M. Mohammad, T. H. Mubarak, and I. H. Mohamed, “Synthesis and characterization of $CoZnFe_2O_4$ ferrite nanoparticles by co-precipitation method for biomedical applications,” Passer Journal of Basic and Applied Sciences, vol. 6, no. 2, pp. 488-493, 2024.

[30] M. A. Issa and K. A. Aadim, “Influence of Laser Energy on Structural and Optical Properties of ZnO(x):NiO(1−x) Films Prepared by Pulse Laser Deposition,” Journal of Optics, 2024.

[31] S. S. Chiad, H. A. Noor, O. M. Abdulmunem, N. F. Habubi, M. Jadan, and J. S. Addasi, “Optical and structural performance of nanostructured Te thin films by (CSP) with various thicknesses,” Journal of Ovonic Research, vol. 16, no. 1, pp. 35-40, 2020.

[32] M. A. Gatou, A. Syrrakou, N. Lagopati, and E. A. Pavlatou, “Photocatalytic TiO_2-based nanostructures as a promising material for diverse environmental applications: a review,” Reactions, vol. 5, no. 1, pp. 135-194, 2024.

[33] A. A. Shihab, “Studying the Physical Properties of Silver Telluride Films Doped with Aluminum by the Effect of Annealing,” Ibn Al-Haitham Journal for Pure and Applied Sciences, vol. 38, no. 1, pp. 121-130, 2025.

[34] M. A. Issa and K. A. Aadim, “Study the structural and optical properties of Zinc Oxide prepared by pulse laser deposition,” Journal of Optics, 2024.

[35] R. Khan, N. Rahman, A. Prasannan, K. Ganiyeva, S. Chakrabortty, and S. Sangaraju, “Phase transition and bandgap modulation in TiO_2 nanostructures for enhanced visible-light activity and environmental applications,” Scientific Reports, vol. 15, no. 1, 20309, 2025.

[36] T. Gakhar and A. Hazra, “Oxygen vacancy modulation of titania nanotubes by cathodic polarization and chemical reduction routes for efficient detection of volatile organic compounds,” Nanoscale, vol. 12, no. 16, pp. 9082-9093, 2020.

[37] O. A. Chichan, N. F. Habubi, M. S. Othman et al., “The role of lithium doping on the physical properties of nanostructured NiO thin films for applications in optoelectronic devices: theoretical and experimental,” Journal of the Australian Ceramic Society, vol. 62, pp. 309-317, 2026.

[38] E. S. Hassan, A. K. Elttayef, S. H. Mostafa, M. H. Salim, and S. S. Chiad, “Silver oxides nanoparticle in gas sensors applications,” Journal of Materials Science: Materials in Electronics, vol. 30, no. 17, pp. 15943-15951, 2019.

[39] N. A. Alghurabi, T. H. Mubarak, A. K. Judran, and B. A. Hasoon, “Two-stage pulsed laser ablation for the production of Ag@TiO_2 core–shell nanoparticles with enhanced antimicrobial properties: An in silico study,” Plasmonics, vol. 20, pp. 10863-10888, 2025.

[40] X. Zhang, P. Yan, B. Zhao, K. Liu, M. C. Kung, H. H. Kung, et al., “Selective hydrodeoxygenation of guaiacol to phenolics by Ni/anatase TiO_2 catalyst formed by cross-surface migration of Ni and TiO_2,” ACS Catalysis, vol. 9, no. 4, pp. 3551-3563, 2019.

[41] S. V. Rathod, V. U. Magar, S. V. Rajmane, D. R. Sapate, and K. M. Jadhav, “Structural and optical characterization of Mg-doped nickel ferrite thin films,” Journal of Materials Science: Materials in Electronics, vol. 36, no. 3, 191, 2025.

[42] S. K. Muhammad, E. S. Hassan, K. Y. Qader, K. H. Abass, S. S. Chiad, and N. F. Habubi, “Effect of vanadium on structure and morphology of SnO_2 thin films,” Nano Biomedicine and Engineering, vol. 12, no. 1, pp. 67-74, 2020.

[43] M. H. Albanda Al-Timimi, W. H. Abdullah, and M. Z., “Influence of thickness on some physical characterization for nanostructured MgO thin films,” East European Journal of Physics, no. 2, pp. 173-181, 2023.

[44] N. M. Kaawash, A. Almalki, F. K. Alanazi, and H. A. Al-Shamiri, "Enhanced UV photodetection properties of nanostructured ZnO films synthesized via spray pyrolysis using different zinc precursors," Optical Materials, vol. 166, 117201, 2025.

[45] M. I. Sayyed and S. Biradar, "Tuning optical properties and gamma-ray attenuation performance in PbO_2-modified borosilicate glasses," Ceramics International, vol. 51, no. 19, pp. 29344-29353, 2025.

[46] Ganesh, A. K. Gupta, P. P. Kumar, P. S. C. Sekhar, K. Radha, G. Padmanabham, and G. Sundararajan, "Preparation and characterization of Ni-doped TiO_2 materials for photocurrent and photocatalytic applications," The Scientific World Journal, vol. 2012, no. 1, 127326, 2012.

[47] M. T. McDowell, M. F. Lichterman, A. I. Carim, R. Liu, S. Hu, B. S. Brunschwig, and N. S. Lewis, "The influence of structure and processing on the behavior of TiO_2 protective layers for stabilization of n-Si/TiO_2/Ni photoanodes for water oxidation," ACS Applied Materials & Interfaces, vol. 7, no. 28, pp. 15189-15199, 2015.

[48] R. S. Ali, N. A. H. Al Aaraji, E. H. Hadi, K. H. Abass, N. F. Habubi, and S. S. Chiad, "Effect of lithium on structural and optical properties of nanostructured CuS thin films," Journal of Nanostructures, vol. 10, no. 4, pp. 810-816, 2020.

[49] M. G. Mulla and R. K. Pittala, "Fabrication and physicochemical properties of nickel oxide (NiO) thin films," Ceramics International, vol. 51, no. 16, pp. 22255-22265, 2025.

[50] S. Liu, M. Wang, G. Liu, N. Wan, C. Ge, S. Hussain, et al., "Enhanced NO_2 gas-sensing performance of 2D Ti_3C_2/TiO_2 nanocomposites by in-situ formation of Schottky barrier," Applied Surface Science, vol. 567, 150747, 2021.

[51] W. Huang, C. Sivakumar, C. H. Wu, C. W. Lee, W. E. Lee, F. Y. Tsai, and M. S. Ho, "Highly Efficient Room Temperature NO_2 Sensor Using Two-Phase TiOx Heterogeneous Nanoparticles," ACS Applied Materials & Interfaces, vol. 16, no. 8, pp. 10485-10495, 2024.

[52] M. Vasudeva, S. D. Varalakshmi, S. D. George, and V. K. Unnikrishnan, "Engineered liquid-repellent substrate for enhanced Laser-Induced Breakdown Spectroscopy (LIBS) of liquid samples," Applied Surface Science, 166364, 2026.

[53] Xue, W. Sun, Y. Bai, Z. Wang, C. Chen, X. X. Li, et al., "Laser energy modulation in laser-induced breakdown spectroscopy of marine aerosols: unraveling energy-coupling pathways and improving quantitative analysis," Journal of Analytical Atomic Spectrometry, 2026.

[54] Y. You, B. Xue, and J. Riedel, "Enhancement of LIBS plasma in air with organic solvent vapors," Spectrochimica Acta Part B: Atomic Spectroscopy, vol. 236, 107309, 2026.

[55] H. Enayati-Taloobaghi, S. Soltani, M. M. Shahidi, and E. Salahi, "Phase engineering and UV photoresponse of TiO_2 films on Si substrates modified with spatially distributed Au nanoparticles," Journal of Materials Science: Materials in Electronics, vol. 37, no. 2, 155, 2026.

[56] Z. Eldjilali, G. S. H. Thien, Z. N. Ng, B. K. Yap, K. B. Tan, H. A. Murthy, and K. Y. Chan, "Electrochromic performances of TiO_2 nanocrystals thin films for smart glass applications," Thin Solid Films, vol. 815, 140636, 2025.

[57] M. L. Vera, H. D. Traid, A. N. Dwojak, M. R. Rosenberger, and C. E. Schvezov, "Advances in nanostructured TiO_2 coatings for industrial applications," in Industrial Applications of Nanoparticles, CRC Press, pp. 228-255, 2023.

[58] N. Farooq, P. Kallem, Z. ur Rehman, M. I. Khan, R. K. Gupta, T. Tahseen, et al., "Recent trends of titania (TiO_2) based materials: A review on synthetic approaches and potential applications," Journal of King Saud University - Science, vol. 36, no. 6, 103210, 2024.

[59] N. S. Kamarudin, N. N. Yaakob, N. F. Sukor, H. D. Setiabudi, M. A. H. Aziz, and R. Jusoh, "Dual-Role Deep Eutectic Solvent-Assisted Electrosynthesis of TiO_2/KCC-1 for Enhanced Visible-Light Photocatalytic Desulfurization," Arabian Journal for Science and Engineering, pp. 1-20, 2026.

[60] A. J. Ghazai, O. M. Abdulmunem, K. Y. Qader, S. S. Chiad, and N. F. Habubi, "Investigation of some physical properties of Mn doped ZnS nano thin films," in AIP Conference Proceedings, vol. 2213, no. 1, p. 020101, 2020.

[61] S. B. Kim, M. S. Lee, S. Y. Lee, and S. J. Park, "Ni/Cu co-doping engineered TiO_2 for efficient solar-light-driven photocatalytic water treatment," Surfaces and Interfaces, 108292, 2025.

[62] M. K. Rashid, H. J. Mohammed, H. M. Hameed, M. W. Muayad, A. M. Hussien, A. T. Awad, and M. Alharbi, "The effect of titanium dioxide (TiO_2) nanoparticle concentration on the performance of polycrystalline silicon solar cells," Journal of Umm Al-Qura University for Engineering and Architecture, vol. 16, no. 4, pp. 1753-1764, 2025.

[63] R. Özmenteş and A. S. Hassanien, "Characterizations and optical discussions of thermally evaporated titanium dioxide thin films," Journal of Optics, vol. 54, no. 3, pp. 1322-1340, 2025.

[64] İ. Erol, G. Khamidov, R. Uktamjon, T. Davlat, and S. Tillayev, "Enhanced thermal, dielectric, and antimicrobial performance of fluorinated methacrylate and chitosan-based nanocomposites reinforced with TiO_2 nanowires," Cellulose, vol. 32, no. 16, pp. 9429-9450, 2025.

[65] X. Cheng, Y. Liu, W. Zhong, S. Li, Y. Li, Z. Zhao, et al., "An Ultra-Selective and Humidity-Resistant Room-Temperature-Operated NO_2 Sensor Based on Black TiO_2," Advanced Science, vol. 12, no. 41, e09293, 2025.